

Photometric observations of weak-line T Tauri stars

II. *wtt*s in Taurus-Auriga, Orion and Scorpius OB2-2^{*,**}

C. Chavarría-K¹, L. Terranegra², M.A. Moreno-Corral¹, and E. de Lara¹

¹ Instituto de Astronomía, Carretera Tijuana Ensenada km 107, Ensenada B.C., CP. 22860, México

² Osservatorio Astronomico di Capodimonte, Via Moiariello 16, I-80131 Napoli, Italy

Received March 25, 1999; accepted April 11, 2000

Abstract. We present *wby-β* photometry of 116 X-ray flux-selected active stars in the directions of the Orion (40), Taurus-Auriga (58) and Scorpius OB2-2 (18) star forming regions. Additionally, we give near IR *JHK* photometry of 20 active stars in the Taurus-Auriga direction. The program stars were selected from the *ROSAT* All Sky Survey and *EINSTEIN* X-ray surveys and are spectroscopically confirmed weak-line T Tauri stars and weak-line T Tauri star candidates. The photometry confirms the young nature of the program stars and also indicates that a significant fraction of the sample could be foreground objects. The data given here probably represent the largest homogeneous *wby-β* photometric sample of new *WTTS* and *WTTS* candidates. Many objects in the sample are observed photometrically for the first time.

Key words: stars: activity — stars: evolution — stars: pre-main sequence

1. Introduction

Soft X-ray surveys of star forming regions (SFRs), for example of Chamaeleon, Lupus, Taurus and Orion, have revealed groups of low-mass ($M_* \leq 3 M_\odot$) active stars apparently associated with those regions (e.g. Alcalá et al. 1995, 1996; Wichmann et al. 1996; Krautter et al. 1997). These objects have late spectral types (typically G0 or later) and are pre-main sequence (PMS) or young (age $\leq 10^8$ yr) main sequence (MS) stars. They are now known as

Send offprint requests to: e-mail: chavarr@astrosen.unam.mx

* Based on observations collected at the Observatorio Astronómico Nacional in Sierra San Pedro Mártir, Baja California, México.

** Tables 1-4 are also available in electronic form at the CDS via anonymous ftp to cdsarc.u-strasbg.fr (130.79.128.5) or via <http://cdsweb.u-strasbg.fr/Abstract.html>

weak-line T Tauri stars (*WTTS*). *WTTS* are apparently associated with SFRs and, assuming that their distances to the observer are those of their associated regions, one infers their youth from their positions in the H–R diagram. Besides these morphological and photometric properties, the *WTTS* also present key features in their spectra that reveal us their young (age $< 10^8$) nature: they have chromospheric activity ($H\alpha$ and CaII H+K lines in emission, $W(H\alpha) \leq -10 \text{ \AA}$), the photospheric line LiII $\lambda 6708 \text{ \AA}$ is conspicuously present in their spectra) and the stars rotate fast ($v_{\text{rot}} \approx 30 \text{ km s}^{-1}$ or more). A necessary condition to classify these objects as PMS stars is the presence of the Li I feature in excess in the $W(\text{Li})$ versus $\log T_{\text{eff}}$ plane when compared with the upper envelope of the Pleiades stars (e.g. Fig. 12 of Alcalá et al. 1998, hereafter A98). In this case, Lithium has not had enough time to be destroyed in the deeper layers of the convection zone (cf. Bodenheimer 1965). On the other hand, the *WTTS* are mildly masked, if at all, by circumstellar material: they lack (strong) spectral line and continuum (ultraviolet or infrared) emissions that characterize the classical T Tauri stars (*CTTS*), which are believed to be younger (age $\leq 10^7$ yr). *WTTS* are considered the descendants of *CTTS*. However, the criteria for establishing the membership of the *WTTS* to an ongoing star forming region should be taken with caution because of their large spatial distribution ($> 100 \text{ \square}^0$) and because their distance to the observer is, in most cases, unknown.

Although the *EINSTEIN* satellite shed new light on the evolution of these PMS objects, its observations were spatially biased towards the denser parts of the SFRs, where *CTTS* predominate and follow a clumpy pattern. Hence, little or no inference could be drawn about the history of star formation at a cloud scale. The spatially unbiased *ROSAT* All-Sky Survey (RASS) remedies this situation: it yields a spatially complete but flux-limited sample of X-ray sources around a given cloud at about *EINSTEIN*'s sensitivity. Contrary to the spatial

distribution of the *CTTS*, *WTTS* were found to be uniformly distributed over the whole observed area and outnumber the preceding *CTTS* by, at least, a factor of 3. The location of the *WTTS* in the evolutionary sequence has not yet been well established (e.g. Montmerle et al. 1993; Chavarría-K et al. 1995), but in general, stellar activity is considered a quantitative landmark of youth for this type of objects. Since *WTTS* are less active in the *uv*, optical and infrared spectral regions than *CTTS*, the former are considered older than the latter. Consequently, *WTTS* had more time to disperse from their birth sites, explaining, at least partially, their broader and homogeneous spatial distribution. Despite the intrinsic X-ray brightness of the *WTTS*, we are luminosity-limited in their detection. At present, we are constrained to only nearby SFRs ($d < 500$ pc).

Many follow-up studies (optical, mostly spectroscopic) of the *EINSTEIN* and *ROSAT* surveys of nearby SFRs such as Chameleon, Taurus-Auriga, Lupus, Orion and Scorpius-Centaurus have recently appeared in the literature (e.g. Alcalá et al. 1995; Wichmann et al. 1996, 1997; Li & Hu 1998; Magazzù et al. 1997; Krautter et al. 1997; Alcalá et al. 1996, 1998; Walter et al. 1988, 1994; Sciortino et al. 1998 and references therein). Unfortunately, photometric data of many *WTTS* and *WTTS* candidates associated with the regions of interest are lacking or the stars were observed in an unsuitable photometric system (e.g. the photographically-based GSC or satellite-born *V* magnitude estimates, particularly for red stars): the exceptions are the monitoring for light-variability of 58 *WTTS* (and *WTTS* candidates) in Taurus by Bouvier et al. (1997) in Johnson's *B* and *V* passbands, the *uvby- β* photometry of *WTTS* and *WTTS* candidates in Orion by Alcalá et al. (1996, hereafter A96) and the *UBVR_IJHKL* photometry of *WTTS* in Scorpius OB2-2 by Walter et al. (1994, hereafter W94).

In this paper we report and discuss photometric data of X-ray flux selected and confirmed *WTTS* and *WTTS* candidates in the Taurus-Auriga SFR (*uvby- β* and *JHK*, 58 and 20 stars, respectively) and in Scorpius OB2-2 SFR (*uvby- β* , 18 stars). We also extend the photometric sample of *WTTS* in Orion reported by A96 (*uvby- β* , 40 stars). The majority of stars are observed for the first time in this photometric system. The data cover about 74% of the objects on the list by Wichmann et al. (1996, hereafter Wi96), about 36% on the list by A96, and about 46% from the list of *WTTS* and *WTTS* candidates in the Upper Scorpius Association by Wa94, as well as six objects near the runaway O star ζ Oph (Oph1 through Oph6, Walter 1986, see also Terranegra et al. 1994).

In spite of previous spectroscopic, photometric and proper motion studies, the membership of *WTTS* to clusters with ongoing star formation is still an open matter. It is the purpose of this work to cover some of these deficiencies for future analysis and observations.

2. Observations and data analysis

The program stars were taken from the spectroscopic follow-up surveys of *ROSAT* X-ray sources in Orion and Taurus-Auriga SFRs by A96 and Wi96, respectively, and from a study of *EINSTEIN* X-ray sources in Scorpius OB2-2 SFR by Wa94 and of X-ray sources east of the Scorpius-Centaurus-Lupus OB association (Walter 1986, hereafter Wa86). Our *uvby- β* observations complement these previous studies. They avoid systematic errors due to different observers, equipment, calibrations or reduction procedures and represent a homogeneous large photometric sample of *WTTS* and *WTTS* candidates.

For convenience purposes, the spatial distributions of our program stars in Taurus-Auriga and Scorpius OB2-2 association are shown in Figs. 1 and 2, respectively.

2.1. The near IR photometry of Taurus-Auriga stars

The *JHK* photometric data of 20 active stars in Taurus-Auriga as presented in Table 1 were collected with the 2.1 m telescope of the Observatorio Astronómico Nacional in Sierra San Pedro Mártir (SPMO, Baja California (México) in November/December 1992. The telescope was used in the f/27 IR configuration mode with a N₂-cooled InSb diode detector. The chopping frequency was set to 10 Hz and a throw of 30'' in the delta direction and a 14'' diaphragm were used throughout the observing run. The set of standard stars for San Pedro Mártir Observatory given by Tapia et al. (1986) was used here to tie the observations to the standard system (see also Carrasco et al. 1991). At least four standard stars were observed nightly. The photometry was reduced following usual procedures (e.g. Mitchell 1960; Chavarría et al. 2000). Details on the equipment, observing procedures and quality of the resulting photometry are given in A96 (see also references therein and remarks in A98), since the equipment and set of standards used are the same in both works. The standard errors of the IR magnitudes of Table 1 are typically $\sigma_J = 0.03$, $\sigma_H = 0.04$ and $\sigma_K = 0.04$.

2.2. The *uvby- β* photometry of program stars

The *uvby- β* photometry of 116 active PMS stars associated with Orion, Taurus-Auriga and Scorpius OB2-2 SFRs was collected during four observing runs from 1994 to 1996 at SPMO using the *Danish* six channel grating spectrophotometer attached to the *Harold L. Johnson* 1.5 m telescope. The photometer consists of an entrance slit, a grating as its dispersing element, six exit slots and filters that match the Strömgren/Crawford original filters fairly well and six uncooled photomultipliers as light detectors in the photon counting mode. Four channels are used for simultaneous *uvby* observations and two for the β -index measurements (the "wide" and "narrow" H β passbands, which

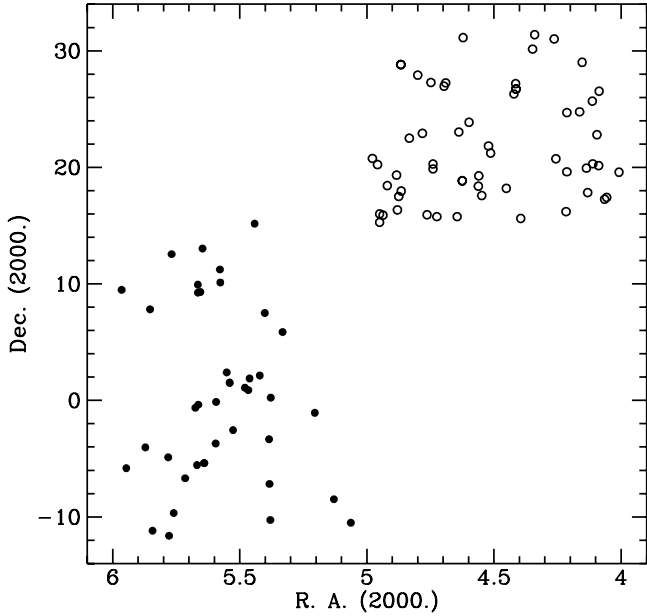


Fig. 1. The spatial distribution of the RASS *WTTS* in Taurus-Auriga (open circle) and in Orion SFRs (filled circle)

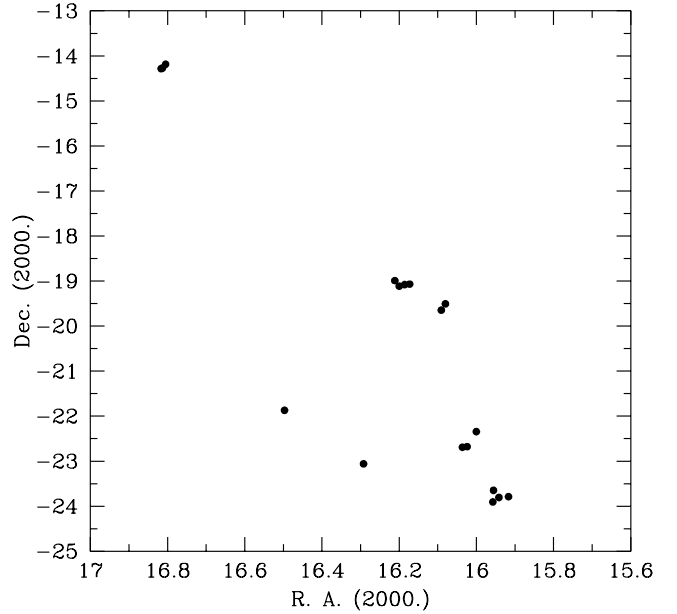


Fig. 2. The spatial distribution of the EO *WTTS* in Scorpius OB2-2

are measured simultaneously). One switches swiftly from one observing mode to the other with a computer command from the data acquisition system. When observing any given star, we made the β -measurements immediately after the *uvby* observations. For more details about the instrument see Nissen (1984); Terranegra et al. (1994, T94 hereinafter) and A96. The integration time on each star was normally fixed in order to achieve a photon noise of less than 1% in the weakest flux of a given passband (usually *u* or *v*). Sky was normally measured 30'' east of the star and, if necessary, intercalated between two 30 second integrations of the star + sky measurements as many times as necessary, until the photon noise error of 1% could be achieved. Some program stars could not be measured with the quoted accuracy. The β index was usually determined with a 2% or better precision. Finally, the seasonal standard stars were each observed twice or more in, at least, one of the four independent runs. The data were reduced to the standard system following usual procedures (e.g. A96, T94, Chavarría et al. 2000). The standard system is taken from the lists by Crawford et al. (1971, 1973) and by Olsen (1983, 1984). On average, about 85 standard stars were observed per season and constitute over 100 standard stars which were used to tie the observations of the different runs to the *uvby- β standard system. We took care to include reference stars covering the spectral types (F5–M5) and luminosity classes (V and III) of the program stars. The resulting *uvby- β photometry of the program stars observed here is displayed in Tables 2 to 4. The typical standard errors for the photometry of the program stars with $V \leq 13^m$ are $\sigma_V = 0.010$, $\sigma_{b-y} = 0.013$, $\sigma_{m1} = 0.015$, $\sigma_{c1} = 0.020$ and $\sigma_\beta = 0.02$ and thrice as large for stars with $V \geq 14^m$.**

3. Results and discussion

3.1. Apparent magnitude distributions

Using the data of Tables 2 to 4 we have compared the apparent *V* magnitude distributions (VD) of *WTTS* with their *CTTS* counterparts in Taurus-Auriga, Orion and Scorpius OB2-2 SFRs. The results are shown in Fig. 3, where the data for the *CTTS* were taken from the Herbig and Bell Catalog (1988) in order to fit the range of spectral types observed: G–M in Orion and K–M in Taurus-Auriga and Scorpius OB2-2. Note that there are no *CTTS* with spectral types earlier than K0 in Taurus-Auriga (cf. Herbig & Bell 1988). The *V*-distribution of Orion's *WTTS* given by us here (cf. Fig. 3a, hatched area) differs from that reported by A98 (their Fig. 2) because our sample covers the weaker end of the stars better. The *V*-distribution of the *WTTS* in Taurus-Auriga is shown in Fig. 3b (hatched area), together with the distribution of the *WTTS* in Scorpius OB2-2 (shaded area) but scaled to the distance of Taurus-Auriga. This was done because of the scarcity of *CTTS* reported in Scorpius OB2-2 (cf. Herbig & Bell 1988).

Again, as in the case of Orion reported by A98, we see that there is a significant number of *WTTS* brighter than the mean brightness of *CTTS*, i.e. the *bona fide* members of the SFRs, indicating us that some of the program stars could be foreground stars. On the other hand, if the objects do belong to the SFR, then many *WTTS* will be more massive and younger than their predecessors, the *CTTS*, in contradiction with the evolutionary scheme for pre-main sequence stars. Many stars would be only a few million years old and, hence, have not had

Table 1. *JHK* photometry of new *WTTS* in Taurus-Auriga

RXJ	<i>J</i>	<i>H</i>	<i>K</i>
0409.3+1716	11.84	11.57	11.49
0412.8+1937	9.88	9.19	9.04
0420.3+3123	10.32	9.74	9.63
0425.3+2618 ¹	9.92	8.62	8.10
0433.7+1823	9.99	9.37	9.27
0433.9+2613 ²	9.65	8.37	7.77
0437.3+3108	10.47	9.58	9.44
0437.5+1851A+B	9.12	8.24	8.10
0441.4+2715	11.05	10.51	10.45
0443.5+1546	10.76	10.11	10.02
0444.4+2017	10.30	9.59	9.47
0444.4+1952	9.60	8.75	8.61
0444.9+2717 ³	7.74	7.22	7.14
0451.9+1758	10.23	9.46	9.27
0452.0+2849A+B	10.70	10.06	9.84
0452.5+1730	9.46	8.43	8.24
0453.0+1920	10.01	9.36	9.22
0456.6+3150 ⁴	7.82	7.16	7.04
0457.5+2014	9.25	8.73	8.59
0458.7+2046	9.55	8.89	9.77

Remarks to table:

¹J4872; ²IT Tau; ³HD 283782 ⁴HD 282598.

the time to disperse. Moreover, one should explain why several *WTTS* get rid of the circumstellar envelope at a faster rate than their predecessors, the *CTTS*. From Fig. 3b we also note that a large fraction of *WTTS* is brighter than the mean brightness of their *CTTS* counterparts. This is more evident if we also consider the large fraction of *WTTS* in Taurus-Auriga with spectral types earlier than K0 (16 stars). One would expect from the stellar evolution theory that the *younger* stars, ie. the *CTTS*, are more luminous than the older *WTTS* (e.g. Shu et al. 1987), in contrast to what we observe in Fig. 3.

The apparent greater brightness of the *WTTS* relative to their *CTTS* counterparts (cf. Fig. 3) could be due to at least three causes: i) *CTTS* are intrinsically fainter than the *WTTS*, ii) *WTTS* are affected by less IS extinction and circumstellar extinction than their *CTTS* counterparts, and iii) *WTTS* are effectively nearer to the Sun than the *CTTS*. In the first case, from a direct comparison between the spectral class distributions of the two types of stars we see a two subclass shift between their respective maxima. This small shift in their spectral types accounts for only about 0^m.5 of the almost 2^m magnitude difference shown in their respective VDs of Fig. 3, minimizing this possibility. With respect to the second case, we do expect, on the average, *CTTS* to be more reddened than their *WTTS* counterparts since the former are masked by circumstellar matter and the latter not. Using the photometry of Tables 2 to 4, the spectral types

Table 2. *wby-β* photometry of the *WTTS* in Orion

RXJ	Sp.T.	<i>V</i>	<i>b - y</i>	<i>m</i> 1	<i>c</i> 1	β	<i>A_V</i>
0503.8-1130	K3	12.26	0.49	0.28	0.23	2.59	0.00
0507.8-0931	K2	12.50	0.55	0.27	0.31	2.59	0.11
0519.9+0552	K6	14.72	0.78	0.58	0.37	2.59	0.36
0522.7+0014†	M2	15.73	1.02	0.63	-0.46	2.43	0.83
0522.8-1144†	M1	14.74	0.97	0.31	-0.30	2.44	0.68
0523.0-0850	K7M0	14.60	0.97	0.41	0.32	2.54	1.02
0523.1-0440	K5	14.68	0.66	0.58	-0.05	2.58	0.00
0524.1+0730	K4	12.72	0.60	0.31	0.37	2.59	0.00
0525.3+0208	M4	15.77	1.00	0.27	0.34	2.42	0.47
0526.5+1510	G5	11.85	0.43	0.20	0.37	2.61	0.15
0527.7+0153†	K7	16.02	0.76	1.00	-0.21	2.69	0.00
0528.0-0053	K0	12.72	0.53	0.37	0.25	2.59	0.31
0528.8+0105	K4	12.67	0.65	0.59	0.27	2.56	0.23
0531.6-0327	K0	9.54	0.56	0.37	0.28	2.58	0.46
0532.4+0131a	K2	11.98	0.51	0.22	0.35	2.60	0.00
0532.4+0131b	K5	13.78	0.70	0.42	0.30	2.58	0.20
0533.1+0224	K4	13.49	0.65	0.38	0.23	2.56	0.23
0534.6+1007	K3	9.91	0.54	0.23	0.29	2.58	0.00
0534.7+1114	K4	12.41	0.51	0.26	0.28	2.58	0.00
0535.6-0152	G9	11.90	0.45	0.21	0.33	2.61	0.00
0535.7-0418†	K3	14.56	0.63	0.81	-0.24	2.49	0.40
0538.4-0637a	K1	12.28	0.63	0.40	0.30	2.58	0.71
0538.4-0637b	K2	12.99	0.58	0.36	0.21	2.55	0.27
0538.8+1302	K2	10.95	0.44	0.19	0.32	2.60	0.00
0539.3+0918	K1	11.71	0.52	0.35	0.28	2.59	0.10
0539.8-0138	K3	13.01	0.67	0.54	0.17	2.58	0.62
0539.9+0915	K0	11.50	0.53	0.32	0.31	2.58	0.31
0539.9+0956	K4	10.91	0.51	0.33	0.27	2.58	0.00
0540.1-0627†	K7M0	15.11	0.78	0.11	-0.14	2.46	0.00
0540.5-0122	K5	10.40	0.33	0.12	0.45	2.65	0.00
0542.9-0719†	M3	14.39	1.07	0.67	0.70	2.47	1.01
0545.6-1020	G7	13.61	1.23	0.22	1.5:	2.59	4.43
0546.1+1233	G9	11.76	0.44	0.18	0.28	2.57	0.00
0546.7-1223	G5	13.30	0.41	0.29	0.34	2.57	0.04
0546.9-0507†	K4	12.30	0.85	0.34	0.26	2.59	1.35
0550.6-1249†	K6	13.43	0.71	0.45	0.78	2.39	0.00
0551.2+0749†	K6	12.35	0.57	0.49	-0.02	2.51	0.00
0552.3-0558	K2	13.09	0.48	0.31	0.16	2.70	0.00
0556.8-0611†	K5	11.84	0.70	0.42	0.19	2.64	0.20
0557.9+0929	G9	11.35	0.42	0.17	0.32	2.60	0.00

Notes to Table:

† After A96, the presence of LiI 6707 Å dubious because of the low S/N ratio of the spectrogram.

reported for the program stars in the literature (A96, Wi96 and Wa94) and the intrinsic colours given by Olsen (1984) we have computed the visual extinction of our program stars. The resulting values are reported in the last column of Tables 2 to 4. We find that the 40 program stars in Orion are reddened, on average, $A_V = 0.36 \pm 0.11$ with a median of 0.13, while the 58 objects in Taurus-Auriga give $A_V = 0.74 \pm 0.09$ with a median of 0.49. Restricting the spectral type ranges of the *CTTS* given by Cohen & Kuhl (1979) to coincide with the spectral types of the program star in Taurus-Auriga and Orion SFRs (mainly K0-K7/M0) and using the A_V estimates for the *CTTS* by Cohen & Kuhl, we find that, on average, the *CTTS* are more reddened by $\delta A_V = 0^m37 \pm 0^m15$ and $= 0^m79 \pm 0^m31$ in Orion and Taurus-Auriga, respectively. Again, this cannot account for the 2^m difference in brightness we observe

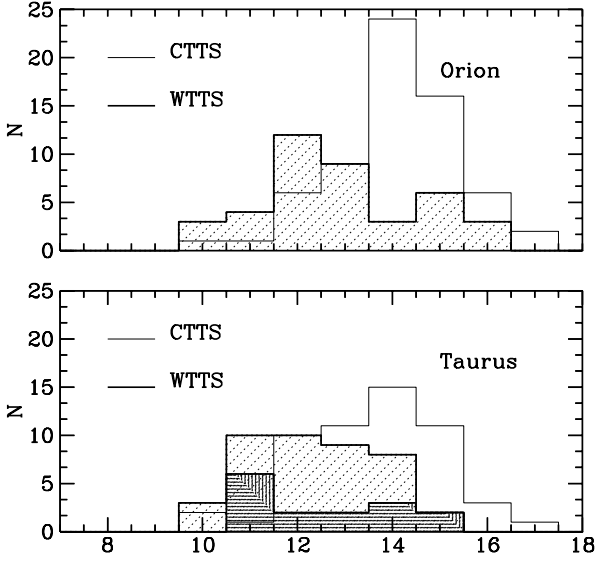


Fig. 3. The apparent V magnitude distributions (VD) of the $WTTs$ studied here. In the upper panel the VD of the program $WTTs$ in Orion (thick line) is compared with that of the $CTTS$ of the same SFR (thin line). In the lower panel we show the VDs of the $WTTs$ and the $CTTS$ in Taurus-Auriga, taken from Herbig & Bell (1988). For comparison we also include the $WTTs$ in Scorpius OB2-2 scaled to the distance of Taurus-Auriga SFR (shaded area). The samples of $CTTS$ were selected in order to fit the range of spectral types observed in Orion (G-M) and in Taurus-Auriga and Scorpius OB2-2 (K-M)

(cf. Fig. 3). Hence, we conclude that, for a given spectral subclass, at least the upper brightest stars in the case of Taurus-Auriga could be foreground objects, the case of Orion being even more obvious.

3.2. Magnitude-colour and two-colour diagrams

In Figs. 4, 5 and 6 we show the observed magnitude V versus colour ($b - y$) diagrams for the program stars associated with Orion, Taurus-Auriga and Scorpius OB2-2, respectively. Also depicted in the figures are the ZAMS from Crawford (1979) and Olsen (1984) scaled to a distance of 460 pc, 140 pc and 160 pc for Orion, Taurus-Auriga and Scorpius OB2-2, respectively. The arrows on the figures indicate the reddening vector. From the location of the program stars in their respective colour magnitude diagram and considering the mean A_V values for the three SFRs, there are indications that the brightest stars could be foreground objects, as mentioned before, others could be reaching the ZAMS and, since they lay below the main sequence at the distance of a given SFR, a few could be background stars.

In Figs. 7 and 8 we show the location of the program stars in the reddening-free ($[m_1]$, $[c_1]$) and the (β , $[m_1]$) diagrams, respectively (Orion filled circles, Taurus-Auriga open circles, Scorpius OB2-2 diamonds). We also show

Table 3. $wby\text{-}\beta$ photometry of the $WTTs$ in Taurus-Auriga

Name/RXJ	Sp.T.	V	$b - y$	m_1	c_1	β	A_V
HD 285281	K1	10.14	0.59	0.31	0.31	2.57	0.49
0403.3+1725	K3	11.69	0.66	0.54	0.12	2.52	0.72
0405.1+2632	K2	11.53	0.55	0.32	0.24	2.55	0.26
0405.3+2009	K1	10.41	0.57	0.36	0.28	2.55	0.22
HD 284135	G3	9.37	0.43	0.12	0.36	2.60	0.31
HD 284149	G1	9.51	0.39	0.11	0.40	2.62	0.18
0406.8+2541	K7M0	11.72	0.87	0.54	-0.11	2.41	1.46
0407.8+1750	K4	11.27	0.52	0.24	0.17	2.53	0.10
0408.2+1956	K2	13.05	0.87	0.14	0.44	2.47	1.74
0409.2+2901	K1	10.64	0.53	0.31	0.26	2.55	0.53
0409.3+1716	M1	13.30	0.95	0.51	0.60	2.54	0.56
0409.8+2446	M1.5	13.30	0.95	0.37	0.27	2.54	0.50
0412.8+1937	K6	12.56	0.81	0.74	-0.03	2.53	0.47
0412.8+2442	G9	11.97	0.76	0.04	0.44	2.60	1.81
HD 285579	G1	10.92	0.50	0.07	0.35	2.65	0.80
0415.4+2044	K0	10.67	0.49	0.20	0.31	2.59	0.30
0415.9+3100	G6	12.36	0.60	0.18	0.30	2.62	1.16
0420.3+3123	K4	11.76	0.60	0.29	0.38	2.61	0.00
0420.9+3009	K7M0	14.74	0.95	0.38	0.82	2.67	0.78
HD 285751	K2	11.25	0.60	0.34	0.31	2.53	0.70
BD+26 718	K1	11.45	0.92	0.12	0.43	2.57	2.33
BD+26 718B	K0	11.47	0.91	0.10	0.47	2.55	2.27
0424.9+2711†	M0.5	13.42	0.89	0.44	-0.38	2.44	0.32
0425.3+2618‡	K7	13.60	1.08	0.12	0.23	2.29	1.76
BD+17 724B	G5	9.44	0.40	0.12	0.37	2.63	0.00
0430.8+2113	G8	10.40	0.47	0.21	0.33	2.59	0.19
HD 284496	K0	10.96	0.52	0.29	0.33	2.59	0.25
0432.8+1735	M2	13.69	1.07	0.48	-0.35	2.40	1.11
0433.5+1916	G6	13.58	0.71	0.16	0.37	2.60	0.56
0433.7+1823	G6	12.05	0.70	0.06	0.42	2.62	1.66
0435.9+2352	M1.5	14.48	1.00	0.35	0.37	2.52	0.72
0437.3+3108	K4	13.80	0.91	0.25	0.41	2.73	2.34
0437.4+1851A	K6	11.84	0.69	0.70	-0.03	2.61	0.00
0437.4+1851B	M0.5	13.45	0.90	0.70	-0.27	2.59	0.50
0438.2+2302	M1	14.42	0.95	0.42	0.39	2.50	0.66
HD 285957	K1	11.05	0.54	0.43	0.28	2.57	0.05
0441.4+2715	G8	13.50	0.81	0.29	0.97	2.88	2.09
HD 283798	G7	9.83	0.40	0.29	0.32	2.60	0.00
0443.4+1546	G7	12.93	0.72	0.14	0.61	2.65	1.59
0444.3+2017	K1	12.66	0.73	0.35	0.23	2.63	1.27
0444.4+1952	M1	12.59	0.93	0.58	0.47	2.58	0.45
0444.9+2717	K1	9.71	0.64	0.25	0.31	2.61	0.77
HD 30171	G5	9.37	0.48	0.23	0.35	2.59	0.43
0446.8+2255	M1	12.94	0.85	0.66	-0.07	2.58	0.00
0447.9+2755	K0	12.39	0.77	—	0.50	2.59	1.77
0450.0+2230	K1	11.08	0.55	0.30	0.27	—	0.26
0451.8+1758	M1.5	14.26	0.98	0.94	0.49	1.95	0.73
0451.9+2849A	K4	14.38	1.00	-0.01	0.76	2.57	2.46
0451.9+2849B	K2	14.52	0.76	0.14	0.52	2.51	1.28
0452.5+1730	K4	12.02	0.64	0.56	0.20	2.56	0.17
0452.8+1621	K6	11.65	0.80	0.60	0.10	2.49	1.07
0452.9+1920	K5	12.15	0.66	0.51	-0.01	2.61	0.00
HD 31281	G1	9.31	0.43	0.13	0.36	2.59	0.40
0456.2+1554	K7	12.77	0.73	0.74	-0.03	2.61	0.00
0457.0+1600	M1	14.42	0.89	0.68	0.00	2.52	0.23
HD 286179	G3	10.34	0.45	0.15	0.31	2.61	0.42
0457.5+2014	K3	11.11	0.53	0.36	0.26	2.61	0.00
0458.7+2046	K7	11.90	0.72	0.84	0.06	2.55	0.00

Notes to Table:

† classified as $WTTs$ by Wichmann (1994).

‡ 04253+2618 SpT. M0, $W(H\alpha) = -2.26 \text{ \AA}$, = J4872.

on the figure the mean ZAMS, giant and sub-giant sequences, adapted from Olsen's (1983, 1984) data for stars with spectral types later than $\approx G2$. In Fig. 8 the lower envelope of the ZAMS (thin solid line), giant and subgiant (β , $[m_1]$) sequences (broken line and thick solid line respectively) are also indicated. We adopted the mean IS reddening law given by Mathis (1990) to obtain the coefficients that define the (reddening-free) colour indices $[m_1]$ and $[c_1]$. For the definition of the indices, see Strömgren

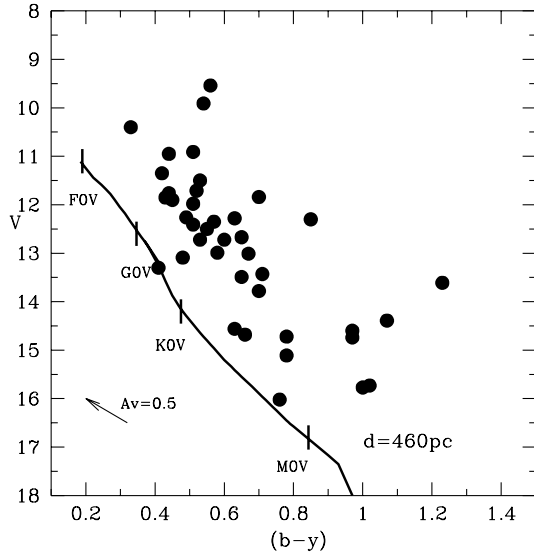


Fig. 4. Colour-magnitude diagram of the *WTTs* in Orion. The ZAMS scaled to the distance of 460 pc is indicated in the figure by the solid line. The direction of the normal reddening vector is also shown in the figure

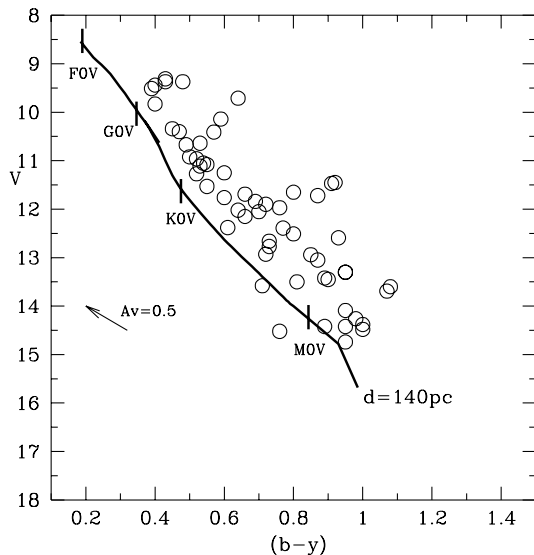


Fig. 5. Colour-magnitude diagram of the *WTTs* in Taurus-Auriga. The position of the ZAMS scaled to the distance of 140 pc is depicted with the solid line

1966 or T94. For the sake of simplicity, in Fig. 8 we plotted only the program stars with spectral types earlier than K7. For later spectral types the reference lines turn to the left in the diagram because of the behaviour of the $[m_1]$ index (cf. Fig. 7).

From a quick inspection of Figs. 7 and 8 it is apparent that, for the later spectral types (G2 or later), the $([m_1], [c_1])$ and $\beta, [m_1]$ diagrams are sensitive to the stellar temperature through the $[m_1]$ index and luminosity- or gravity-dependent through the $[c_1]$ and β indices. Because of this, the $([m_1], [c_1])$ diagram is an observational HR-diagram but with the advantage that it is distance- and reddening-independent. One further infers that a large

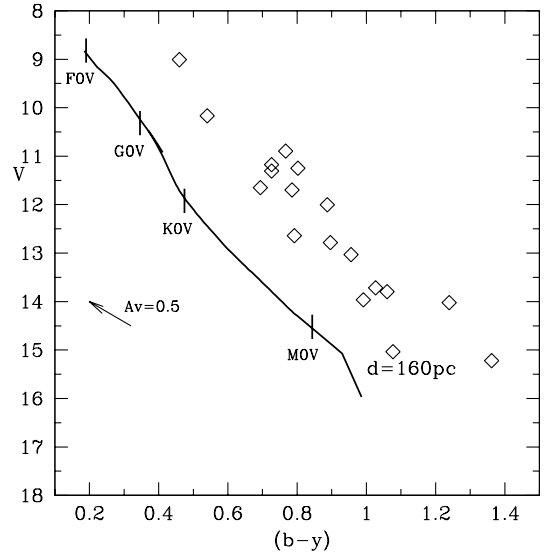


Fig. 6. Colour-magnitude diagram of the *WTTs* in Scorpius OB2-2 and Ophiuchus. The position of the ZAMS scaled to the distance of 160 pc is shown with the solid line

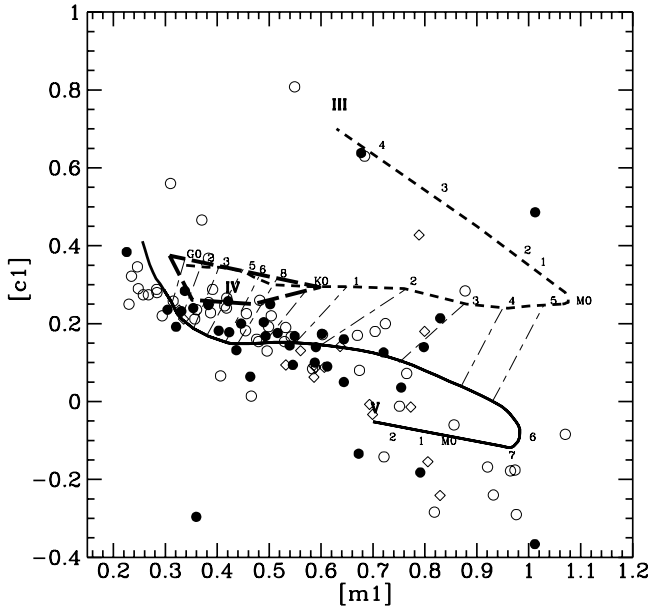
fraction of the program stars are colder and less gravitative than their dwarf counterparts, with an upper limit for the temperature $T_{\text{eff}} \leq 6500$ K (spectral type F6 or later) and hence lie in the expected domain for young stars with enhanced $\text{LiI } \lambda 6708 \text{ \AA}$ absorption. Five stars seem to have gravities suitable of giant stars (cf. Fig. 7). A large fraction of the sample stars typically have luminosity class between III and V but the diagrams show a large scatter, with many stars out of bounds. This was due to i) the fact that, originally we wanted only to obtain the magnitude V and the color $(b-y)$ of the program stars, in order to deredden the data and fix the stars in a luminosity-temperature diagram using bolometric corrections and ii) that some program stars still suffer of veiling, making their $[c_1]$ and $[m_1]$ indices bluer than expected for their spectral class. We also make the remark that the c_o and m_o color indices were obtained as a byproduct since the photometer measures all four filter bands simultaneously. The composed colours should be measured more accurately to be conclusive, particularly for late type stars. In any case, one should be aware that an error of 0.2 in the $[m_1]$ index causes a classification error of two spectral subclasses, but the same error in $[c_1]$ leads to a difference between a giant and a dwarf star. Anyhow, this result for the sample reassures us that many program stars are PMS objects. We also note that the sample in Taurus-Auriga is hotter than the sample in Orion.

From Fig. 8 it is also apparent that some stars scatter all over the diagram, mimicking gravitative objects, stars with strong winds or stars with $\text{H}\beta$ filled-in with emission or in emission. The program stars with $\text{H}\alpha$ in emission from the literature, are indicated with crosses in the figure. We conclude that little or no additional information can be drawn from the location of the program stars in Fig. 8.

Table 4. *uvby-β* photometry of *WTTS* in Scorpius OB2-2 and in Ophiuchus

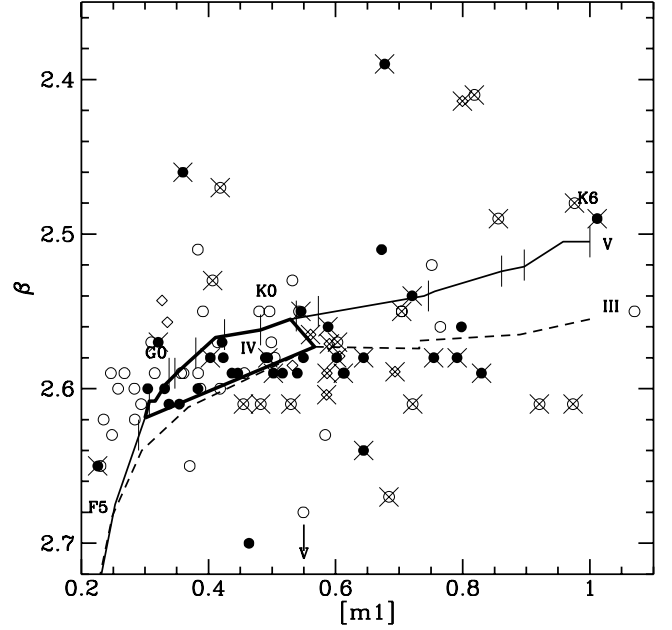
Name/RXJ	Sp.T.	<i>V</i>	<i>b-y</i>	<i>m1</i>	<i>c1</i>	β	<i>A_V</i>
155203–2338	G2IV	9.01	0.46	0.19	0.30	2.56	0.48
155331–2340	M1.5	13.03	0.96	0.47	0.18	2.64	0.53
155421–2330	M0	12.78	0.90	0.69	-0.24	2.54	0.48
155427–2346	M0.5	13.80	1.06	0.36	0.18	2.59	1.27
155703–2212	M1	13.72	1.03	0.48	0.05	2.61	0.99
155828–2232	K1IV	11.65	0.69	0.37	0.23	2.57	1.07
155913–2233	K5IV	11.31	0.73	0.46	0.14	2.59	0.34
160153–1922	K2IV	11.17	0.73	0.37	0.23	2.58	1.09
160233–1931	M1	13.96	0.99	0.51	-0.04	2.66	0.79
160728–1856	M1	15.03	1.08	0.29	0.36	2.75	1.27
161431–2256	G0IV	10.17	0.54	0.15	0.34	2.54	1.08
162649–2145	K0IV	11.25	0.80	0.30	0.29	2.56	1.83
Oph1	K2	12.00	0.89	0.30	0.27	2.60	1.99
Oph2	K1	11.70	0.79	0.28	0.25	2.58	1.58
Oph3	K0	10.89	0.77	0.34	0.22	2.59	1.63
Oph4	K4	14.0	1.24	0.4	0.43	2.41	3.52
Oph5†	M2	15.22	1.36	0.35	0.70	2.87	0.15
Oph6†	K7	12.64	0.79	-0.12	-1.5 : 2.75	2.74	

Notes to table: † CTTS, after Wa88.


Fig. 7. The $([m_1], [c_1])$ diagram of the *WTTS* in the SFRs studied: Orion (filled circle), Taurus-Auriga (open circle), Scorpius OB2-2 (diamond). The thick line represents the ZAMS

From the spectral types of the program stars given in the literature and the photometric indices given here we also conclude that the $[m_1]$ colour index enables us to give a good stellar temperature estimate T_* for the program stars (typically within a subclass). We also find that the program stars are for the most part about half a spectral subclass colder than their main-sequence counterparts.

In Fig. 9 we show the equivalent width $W(\text{H}\alpha)$ as a function of the β index for the program stars. The β data were taken from Tables 2, 3 and 4 of this work and the $W(\text{H}\alpha)$ data were taken from A96, Wi96 and Wa94. Also shown in the figure is the expected relation between β and


Fig. 8. The $(\beta, [m_1])$ -diagram of the *WTTS*. Symbols as Fig. 7. For clarity, only the *WTTS* earlier than K7 are plotted in the figure. The program stars with $\text{H}\alpha$ in emission are indicated with crosses

$W(\text{H}\alpha)$ for dwarfs (dotted line) and giants (solid line). The $W(\text{H}\alpha)$ values for the reference lines were obtained by measuring the equivalent width of the $\text{H}\alpha$ line for a suitable sample of dwarf and giant stars selected from the library of spectra by Montes et al. (1997), while the β values were obtained from Hauck & Mermilliod (1998). From the figure we notice that, besides the fact that the β and $W(\text{H}\alpha)$ values were not determined simultaneously for stars with $\text{H}\alpha$ in emission, the β index is usually also indicative of emission. From Fig. 9 we also conclude that most of our sample stars have $\text{H}\alpha$ filled-in or in emission.

Sixteen of the eighteen *WTTS* with a photometric rotational period studied by Bouvier et al. (1997) are contained in our sample of program stars in Taurus. In general, their visual magnitudes coincide with our values within the observational errors and the intrinsic variability of the objects in common ($\delta V(\text{ours} - \text{bou97}) = +0^{\text{m}}049$, $\sigma_{\delta V} = 0.091$), except for RXJ0420.3+3123: this star deviates by more than $\delta V = -0^{\text{m}}57$. Its range of variability is found to be only $0^{\text{m}}07$ (cf. Bouvier et al. 1997). Excluding this star, we expect to obtain the same physical parameters for the subsample of stars in common with Bouvier et al. (1997), such as A_V , T_{eff} , $\log(L_*/L_\odot)$, τ_{age} , etc., if we assume that they all belong to the Taurus-Auriga SFR. We find a similar situation for the *WTTS* associated with the Scorpius OB2-2 association, since our data matches that of Wa86 and Wa94, except for two of the objects: Oph6 and RXJ155703-2212. Oph6 is a *CTTS* and its range of variations can be larger than that quoted by Wa94; RXJ155703-2212 is almost $0^{\text{m}}5$

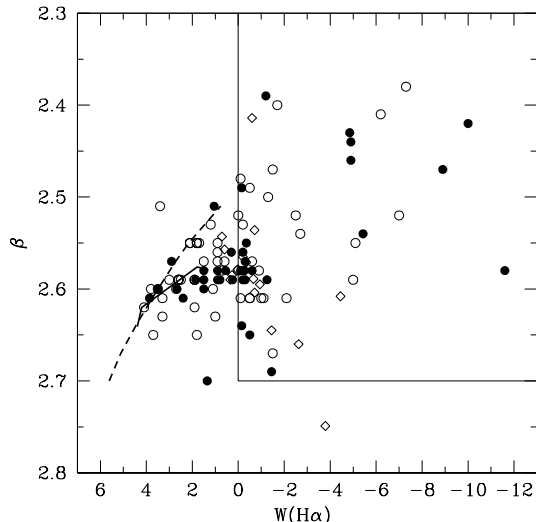


Fig. 9. The β vs. $W(H\alpha)$ -diagram of the *WTTS*. The dotted and the solid lines represent the expected β vs. $W(H\alpha)$ relations for dwarf and giant stars respectively. The filled and open circles represent the sample stars in Orion and Taurus-Auriga, respectively. The diamonds represent objects in Scorpius OB2-2 and Ophiuchus. For more details, consult Sect. 3.2.2

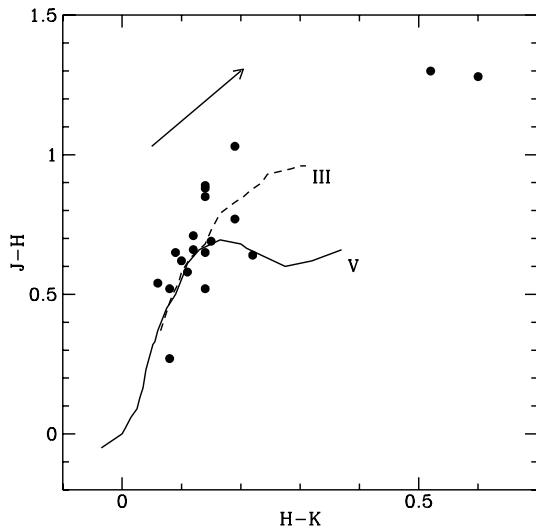


Fig. 10. The $(J - H)$ vs. $(H - K)$ diagram for the *WTTS* in Taurus-Auriga. The solid line is the location of the main sequence and the broken line the giant sequence, adapted from the data given by Bessell & Brett (1988). The arrow indicates the direction of the (normal) reddening vector

fainter now than its brightness given by Wa94 earlier. We find no clear explanation for this change.

However, as mentioned before in Sects. 3.1 and 3.2, some of the program stars can be foreground objects and a better distance estimate for these stars is required in order to derive their physical parameters. The $uvby-\beta$ photometry given here provides such a possibility (Terranegra & Chavarría-K 1999).

Figure 10 shows the location in the two-colour ($J - H$, $H - K$) diagram of the *WTTS* in Taurus-Auriga. Also given in the figure are the loci of the main (solid line) and giant (broken line) sequences, taken from Bessell & Brett (1988). One readily sees from Fig. 10 that, except for two stars which are highly reddened with an apparently normal IS extinction law, namely the *CTTS* RXJ0433.9+2613 (*IT Tau*) and RXJ0425.3+2618 (J4872), the rest of the *WTTS* have, within the observational errors, similar IR colors to those of normal field dwarf stars later than K2. A more detailed examination of the program stars with optical and IR photometric data indicates that, on average, the *WTTS* have a slight near IR excess, probably due to a remnant of circumstellar matter. Finally, integrating under the dereddened (broad) spectral flux distribution derived from the near IR and optical data of 19 stars in Taurus-Auriga in order to calculate their bolometric luminosity, we confirm Wa94's result that the stars follow, within the observational errors ($\sigma(L_*) \leq 0.1$ dex), the bolometric correction relations for dwarfs and giants (e.g. Schmidt-Kaler 1982). Thus, luminosities derived from the dereddened visual magnitude and colour using bolometric corrections are good estimates for our purposes.

In conclusion, in this work we show, independently of any distance estimate, that, in general, the program stars are more luminous than ZAMS stars, typically with luminosity classes between III and V (cf. the $([m_1], [c_1])$ and $(\beta, [m_1])$ diagrams), giving support to the premise that they are young (PMS) objects and in agreement with their activity indicators provided by the spectroscopy. Another important result is that the *WTTS* and *WTTS* candidates are a mixture of objects belonging to the SFRs studied here and of foreground and yet young (i.e. PMS) stars, since they still do not reach the main sequence. Some objects are too far from the assumed parent SFR to be explained by isotropic drifting or slingshot mechanisms (cf. Herbig 1978; Sterzik & Durisen 1995, respectively). Some of the stars could belong to the Gould Belt population or, less probably, they were formed locally (cf. Guillout et al. 1998; Feigelson 1996, respectively).

Much observational work still has to be done in order to elucidate their true nature and $uvby-\beta$ is one of the techniques that enables us to answer some of these matters.

Acknowledgements. We thank Juan Manuel Alcalá and Rainer Wichmann for making many program stars in Orion and Taurus-Auriga regions available to us prior to their publication. We appreciate the useful comments and suggestions by the referee, R. Wichmann, Juan Manuel Alcalá and Michael Sterzik for interesting and fruitful discussions about *WTTS*, and the technical and administrative staff of SPMO for their continuous and enthusiastic support in the realization of the observing runs. C. Chavarría-K thanks Prof. M. Capaccioli for making his stay at the OAC-Napoli possible. Christine Harris proofread the manuscript.

This work was partially supported by Consejo Nacional de Ciencia y Tecnología, México (projects 400340-4-2243 PE and 400354-5-27757 E), and by the CNR-GNA98 and COFIN98-MURST, Italy.

References

- Alcalá J.M., Krautter J., Schmitt J.H.M.M., Covino E., Wichmann R., Mundt R., 1995, *A&AS* 114, 109
- Alcalá J.M., Terranegra L., Wichmann R., et al., 1996, *A&AS* 119, 7 (A96)
- Alcalá J.M., Terranegra L., Chavarría-K C., 1998, *A&A* 330, 1017 (A98)
- Bessell M.S., Brett J.M., 1988, *PASP* 100, 1134
- Bodenheimer P., 1965, *ApJ* 142, 459
- Bouvier J., Wichmann R., Grankin K., et al., 1997, *A&A* 318, 495
- Carrasco L., Recillas-Cruz E., García-Barreto A., et al., 1991, *PASP* 103, 987
- Chavarría A., de Lara E., Chavarría-K C., 2000, *ArcoIris.v02* (RainBow.v02), a multiwavelength reduction program for IBM compatible PC's. Instituto de Astronomía, U.N.A.M., México
- Chavarría-K C., Moreno-Corral M.A., de Lara E., 1995, *Rev. Mex. Astron. Astrofis. (Suppl.)* 3, 117
- Cohen M., Kuhl L.V., 1979, *ApJS* 41, 743
- Crawford D.L., 1979, *AJ* 84, 1858
- Crawford D.L., Barnes J.V., Golson J.C., 1971, *AJ* 76, 1058
- Crawford D.L., Barnes J.V., Golson J.C., Hube D.P., 1973, *AJ* 78, 738
- Feigelson E.D., 1996, *ApJ* 468, 306
- Guillout P., et al., 1998, *A&A* 337, 113
- Hauck B., Mermilliod M., 1998, *A&AS* 129, 431
- Herbig G.H., 1978, in *Problems of physics and evolution of the Universe*, Miroyan L. (ed.). Academy of Science of Armenia, Erevan, p. 171
- Herbig G.H., Bell K.R., 1988, *Lick Obs. Bull. No.* 1111
- Krautter J., Wichmann R., Schmitt J.H.M.M., et al., 1997, *A&AS* 123, 329
- Li J.Z., Hu J.Y., 1998, *A&AS* 132, 173
- Maggazù A., Martín E.L., Sterzik M.F., Neuhäuser R., Covino E., Alcalá J.M., 1997, *A&AS* 124, 449
- Mathis J.S., 1990, *ARA&A* 28, 37
- Mitchell R., 1960, *ApJ* 132, 68
- Montes D., Martín E.L., Fernández-Figueroa M.J., Cornide M., De Castro E., 1997, *A&AS* 123, 473
- Montmerle Th., Feigelson F.D., Bouvier J., André P., 1993, *Protostars and Planets III*, Levy E., Lumine J. (eds.). University of Arizona Press, p. 689
- Nissen P.E., 1984, *User's manual of the Danish uvby- β photometer*. Instituto de Astronomía, México
- Olsen E.H., 1983, *A&AS* 54, 55
- Olsen E.H., 1984, *A&AS* 57, 443
- Sciortino S., Damiani F., Favata F., Micela G., 1998, *A&A* 332, 825
- Schmidt-Kaler T.H., 1982, in *Physical parameters of stars*, Landolt-Börnstein New Series, Vol. 2b, Astronomy and Astrophysics, Stars and Clusters, Schaifers K., Voigt H.H. (eds.). Springer Verlag, New York
- Shu F.H., Adams F.C., Lizano S., 1987, *ARA&A* 25, 23
- Sterzik M.F., Durisen R.H., 1995, *A&A* 304, L9
- Strömgren B., 1966, *ARA&A* 4, 433
- Tapia M., Neri L., Roth M., 1986, *Rev. Mex. Astron. Astrofis.* 13, 115
- Terranegra L., Chavarría-K C., Diaz S., González-Patiño D., 1994, *A&AS* 104, 557 (T94)
- Terranegra L., Chavarría-K C., 1999, in "Second Three-Islands Euroconference on Stellar Clusters and Associations: Convection, Rotation and Dynamos", Mondello, Palermo, Italy
- Walter F.M., 1986, *ApJ* 306, 573 (Wa86)
- Walter F.M., Brown A., Mathieu R.D., Myers P.C., Vrba F.J., 1988, *AJ* 96, 297 (Wa88)
- Walter F.M., Vrba F.J., Mathieu R.D., Brown A., Myers P.C., 1994, *AJ* 107, 692 (Wa94)
- Wichmann R., 1994, Ph.D. Dissertation, Heidelberg, Germany
- Wichmann R., Krautter J., Schmitt J.H.M.M., et al., 1996, *A&A* 312, 439 (Wi96)
- Wichmann R., Krautter J., Covino E., Alcalá J.M., Neuhäuser R., Schmitt J.H.M.N., 1997, *A&A* 320, 185